Dye

اونيۏرسيتي تيكنولوݢي مارا
UNIVERSITI TEKNOLOGI MARA

University Publication Centre (UPENA)

Journal of Mechanical Engineering

An International Journal

Volume 7 No. 2 December 2010 ISSN 1823-5514

JOURNAL OF MECHANICAL ENGINEERING (JMechE)

Journal of Mechanical Engineering (ISSN 1823-5514) is jointly published by the Faculty of Mechanical Engineering (FKM) and Pusat Penerbitan Universiti (UPENA), Universiti Teknologi MARA, 40450 Shah Alam, Selangor, Malaysia.

Journal of Mechanical Engineering

An International Journal

Volume 7 No. 2 December 2010 ISSN 1823-5514

Modelling of Belt-Driven High-Speed Laser Beam Manipulator

Muhammad Azmi Ayub
Faculty of Mechanical Engineering
Universiti Teknologi MARA (UiTM) Malaysia
Email: muhammadayub@salam.uitm.edu.my

Pavel Hynek
Mike Jackson
Mechatronic Research Centre
Loughborough University United Kingdom

ABSTRACT

This paper deals with a linear belt-driven servomechanism in the development of high-speed laser beam manipulator. The objectives of this paper are to accurately model the belt-driven mechanism and determine its resonance frequencies, phase margin and bandwidth. The use of timing belt to convert rotary to linear motion provides a cost-effective solution that can achieve high agility, high efficiency and long travel distance. However, the use of belt-drive causes uncertain dynamic behaviour and resonance problems because of its elasticity that leads to vibrations, compliance, and higher friction. Consequently, complex control strategies are required for effective control of the laser-beam trajectory planning. To reduce these problems, a complete information about system dynamics of the belt-driven mechanism is required and a comprehensive state-space model of belt-driven servomechanism is developed and presented in this paper. Frequencies response approach is used to determine the resonance for accurate control strategy of the manipulator trajectory planning.

Keywords: *Belt-drive, modelling, high-speed, laser manipulator, system dynamic, resonance, bandwidth.*

ISSN 1823-5514

Nomenclature

T_m	Motor torque
T_f	Torque due the friction inherent in the mechanism.
J_o	Moment inertia of rotor and motor gear
R_o	Radius of motor gear
C_o	Viscous damping coefficient of motor
θ_o	Angular displacement of motor shaft
T_1	Torque at the driving pulley shaft gear
J_1	Moment inertia of driving pulley gear
R_1	Radius of driving gear
C_1	Viscous damping of the driving gear
θ_1	Angular displacement of driving gear
J_2	Moment inertia of driving pulley and gear
R_2	Radius of driving pulley
C_2	Viscous damping of the driving pulley
θ_2	Angular displacement of the driving pulley
J_3	Inertia of driven pulley and slide carriage
R_3	Radius of driven pulley
C_3	Viscous damping of the driven pulley
θ_3	Angular displacement of driven pulley
K_b	Stiffness of timing belt
T_o	Load torque on the motor gear due to the rest of the driving mechanism.
C_b	Damping coefficient of the timing belt
R_p	Radius of driving and driven pulley
M	Mass of the laser head
F_a	Force at the tight tension of timing belt
F_b	Force at the slack tension and of timing belt
F_i	Pre-set initial tension of the timing belt
E	Young Modulus of the belt
A	Cross-sectional area of timing belt
L	Length of timing belt
L_a	Armature inductance of DC-Motor
R_a	Armature resistance of DC-Motor
T_m	Torque of DC-Motor
K_m	Torque constant
i_a	Armature current
E_b	Back EMF
E_a	Armature voltage
K_e	Back EMF constant

Introduction

Several possible concept of 2D laser-beam manipulators for high-speed laser cutting machines have been developed by researchers [1, 2, 3]. In general, most of these concepts are designed not for cutting web materials which is thin and long materials such as web plastic, web fabric or web metal. Therefore, a new concept of the laser manipulator is proposed as shown in Figure 1 [4]. The laser beam manipulator employs one mirror with single-revolute and single-prismatic joint. This configuration can be achieved by mounting a scanner mirror to a four-wheel carriage. A dynamic focussing lens or flat-field scan lens is used in conjunction with this laser-beam manipulator. To ensure high rigidity of the laser-beam manipulator, the four-wheel carriage is mounted to a linear slide, which consists of two rectangular bars fitted with tracks. The scanner mirror is inclined at 45 degrees with respect to the linear movement of the slide. The mirror itself can rotate with respect to the axis of the scanner. A timing belt-mechanism is used to drive the linear motion of the slide in the x-direction which is the length of the timing belt needs to drive the laser head along the web materials. The movement of this timing-belt is driven by a geared servomotor, which is coupled with the pulley at the one end of the liner slide. In the y-direction, the rotational motion θ_y, of the mirror can be actuated by the scanner. Hence, the trajectory of the laser beam can be controlled in the x-direction by the linear slide and in the y-direction by the rotational motion of the mirror. To monitor the position, the pulley at the other end of the linear slide is fitted with an optical encoder.

The use of timing belt in the drive mechanism provides a long stroke and cost-effective solution for the motion of laser beam in the x-direction at high speed, high agility and high efficiency [5]. However, the use of belt-drive causes uncertain dynamic behaviour and resonance phenomena because of its elasticity that leads to vibrations, compliance, and higher friction [6]. Consequently, belt-driven mechanism suffers from complicated control strategies in order to achieve high precision and accuracy of trajectory planning. A robust position control strategies such as sliding mode control can suppresses vibrations due to resonance and assures wide system bandwidth for high accuracy, high precision and rapid laser beam manipulation [7, 8, 9]. Alternatively, simple PID control strategy can be used as long as the resonance is outside the system bandwidth [10]. To implement these control strategies requires complete information about system dynamics of the belt-driven mechanism. Therefore, in order to attain higher performance laser beam manipulator, a more accurate model of

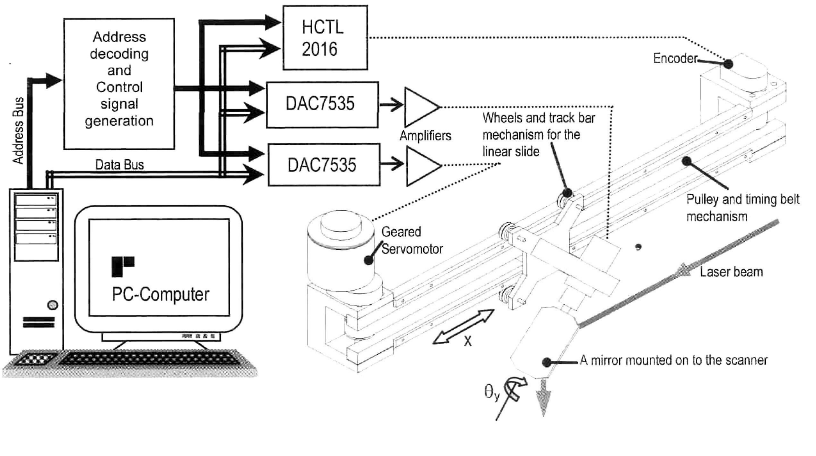

Figure 1: Belt-Driven Servomechanism of High-Speed Laser Beam Manipulator System

belt-driven mechanism is desired. This comprehensive dynamic model can be used to determine important parameters, such resonance, phase margin and stability of the system, for accurate control strategy of the laser-beam trajectory planning.

Mathematical Modelling of the Dynamics System

As mentioned earlier, the laser-beam manipulator is driven by a timing belt and pulley mechanism to move the laser head laterally or longitudinally across the cutting table. This mechanism can be represented as inter-connected standard components of mass, springs and dampers, as shown Figure 2. It is assumed that the stiffness of the shafts is infinite for relatively small inertia load and the numbers of teeth on each gear are proportional to the radius of the gear for the gears to engage properly. There is neither backlash nor elastic deformation on the gear nor slip between the belt and the pulleys. With these assumptions the laser beam manipulator can be considered as two degrees of freedom system. By applying Newton's second law of motion, two fundamental equations of motion to describe the dynamic behaviour of the system can be derived.

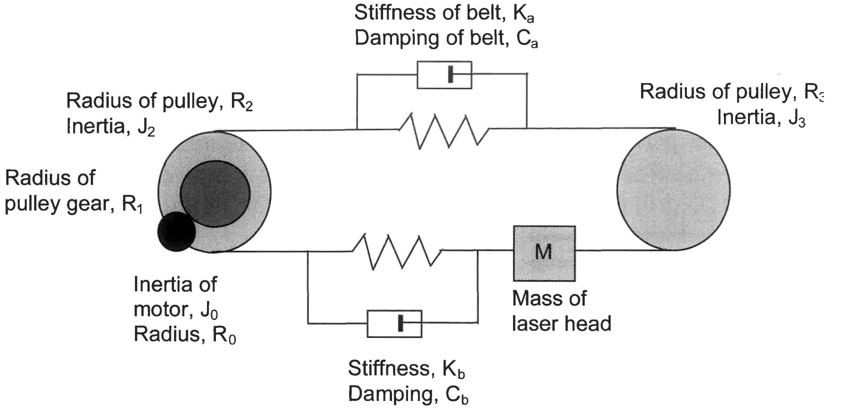

Figure 2: Model of the Laser-Beam Manipulator

The first equation of motion is for the driving pulley shaft at which the torque of the motor shaft is applied. The basic equation (1) at the motor driving shaft is as follows

$$T_m = T_o + T_f + C_0 \frac{d\theta_0}{dt} + J_0 \frac{d^2\theta_0}{dt^2} \tag{1}$$

The equation of motion for the torque transmitted to the driving pulley shaft can be written as follows,

$$T_1 = R_2(F_a - F_b) + C_2 \frac{d\theta_2}{dt} + J_2 \frac{d^2\theta_2}{dt^2} \tag{2}$$

The force F_i is the initial pretension force of the belts. F_a and F_b are forces due to the tight and slack belts tension respectively. These two forces as a result of the elasticity of the timing belt can be expressed as follows,

$$F_a = F_i + \left[K_a \Delta(t) + C_a \frac{d\Delta(t)}{dt} \right] \tag{3}$$

$$F_b = F_i - \left[K_b \Delta(t) + C_b \frac{d\Delta(t)}{dt} \right] \tag{4}$$

where elongation of belt, $\Delta(t) = R_2\theta_2(t) - R_3\theta_3(t)$

It is designed that the radius of both pulleys are identical and that the stiffness and damping coefficient of the tight and slack belt tension are identical. Hence the following design simplifications can be made: the radius of both pulleys, $R_p = R_2 = R_3$; the damping coefficient of belt, $C_a = C_b$; and the stiffness coefficient of belt, $K_a = K_b$.

From equation (3) and (4) above, the difference in tension force between the tight and slack belt can be obtained and deduced as follows,

$$F_a - F_b = 2\left[K_b \Delta(t) + C_b \frac{d\Delta(t)}{dt} \right]$$

$$F_a - F_b = 2\left[K_b (R_p\theta_2 - R_p\theta_3) + C_b (R_p \frac{d\theta_2}{dt} - R_p \frac{d\theta_3}{dt}) \right] \tag{5}$$

$$F_a - F_b = 2R_p\left[K_b (\theta_2 - \theta_3) + C_b (\frac{d\theta_2}{dt} - \frac{d\theta_3}{dt}) \right]$$

Substitute equation (5) into (2), produce the following equation (6),

$$T_1 = 2R_p^2 \left[K_b (\theta_2 - \theta_3) + C_b (\frac{d\theta_2}{dt} - \frac{d\theta_3}{dt}) \right] + C_2 \frac{d\theta_2}{dt} + J_2 \frac{d^2\theta_2}{dt^2} \tag{6}$$

If there is no power loss through the mechanism, $T_0 = \frac{T_1}{R_1} R_0$

Eliminating T_0 and T_1 from equation (1) and equation (6), yields

$$T_m = \frac{T_1}{R_1} R_0 + T_f + C_0 \frac{d\theta_0}{dt} + J_0 \frac{d^2\theta_0}{dt^2}$$

$$T_m = \frac{R_0}{R_1}\left[2R_p^2 \left[K_b(\theta_2 - \theta_3) + C_b(\frac{d\theta_2}{dt} - \frac{d\theta_3}{dt}) \right] + C_2 \frac{d\theta_2}{dt} + J_2 \frac{d^2\theta_2}{dt^2} \right]$$

$$+ T_f + C_0 \frac{d\theta_0}{dt} + J_0 \frac{d^2\theta_0}{dt^2} \qquad (7)$$

Substituting variables $\theta_2 = \frac{R_0}{R_1}\theta_0$ and $\theta_2 = \theta_1$ into the above equation (7) and simplifying the equation, will give the first final equation of motion for the system

$$T_m = \frac{R_0}{R_1}\left[2R_p^2 \left[K_b(\frac{R_0}{R_1}\theta_0 - \theta_3) + C_b(\frac{R_0}{R_1}\frac{d\theta_0}{dt} - \frac{d\theta_3}{dt}) \right] + C_2 \frac{R_0}{R_1}\frac{d\theta_0}{dt} + \right.$$

$$\left. J_2 \frac{R_0}{R_1}\frac{d^2\theta_0}{dt^2} \right] + T_f + C_0 \frac{d\theta_0}{dt} + J_0 \frac{d^2\theta_0}{dt^2}$$

$$T_m = 2R_p^2\ K_b(\frac{R_0}{R_1})^2\theta_0 - 2R_p^2\ K_b(\frac{R_0}{R_1})\theta_3 + 2R_p^2\ (\frac{R_0}{R_1})^2 C_b \frac{d\theta_0}{dt} -$$

$$2R_p^2\ C_b(\frac{R_0}{R_1})\frac{d\theta_3}{dt}) + C_2(\frac{R_0}{R_1})^2 \frac{d\theta_0}{dt} + J_2(\frac{R_0}{R_1})^2 \frac{d^2\theta_0}{dt^2} + T_f +$$

$$C_0 \frac{d\theta_0}{dt} + J_0 \frac{d^2\theta_0}{dt^2}$$

$$T_m = T_f + 2R_p^2\ K_b(\frac{R_0}{R_1})^2\theta_0 + \left[(\frac{R_0}{R_1})^2[C_2 + 2R_p^2\ C_b] + C_0 \right]\frac{d\theta_0}{dt}$$

$$- 2R_p^2\ K_b(\frac{R_0}{R_1})\theta_3 - 2R_p^2\ C_b(\frac{R_0}{R_1})\frac{d\theta_3}{dt}$$

$$+ \left[J_0 + J_2(\frac{R_0}{R_1})^2 \right]\frac{d^2\theta_0}{dt^2} \qquad (8)$$

Similarly, the second equation (9) of motion for the driven pulley can be formulated as follows,

$$R_3(F_a - F_b) + C_3\frac{d\theta_3}{dt} + J_3\frac{d^2\theta_3}{dt^2} = 0 \tag{9}$$

Substitute equation (5) into (9), yields

$$R_3\left[2R_p\left[K_b(\theta_2 - \theta_3) + C_b(\frac{d\theta_2}{dt} - \frac{d\theta_3}{dt})\right]\right] + C_3\frac{d\theta_3}{dt} + J_3\frac{d^2\theta_3}{dt^2} = 0$$

$$2R_p^2\left[K_b(\theta_2 - \theta_3) + C_b(\frac{d\theta_2}{dt} - \frac{d\theta_3}{dt})\right] + C_3\frac{d\theta_3}{dt} + J_3\frac{d^2\theta_3}{dt^2} = 0 \tag{10}$$

Substituting the variables $\theta_2 = \frac{R_0}{R_1}\theta_0$ and $\theta_2 = \theta_1$ into the above equation (10) and simplifying the equation, yields the following equation,

$$2R_p^2\left[K_b(\frac{R_0}{R_1}\theta_0 - \theta_3) + C_b(\frac{R_0}{R_1}\frac{d\theta_0}{dt} - \frac{d\theta_3}{dt})\right] + C_3\frac{d\theta_3}{dt} + J_3\frac{d^2\theta_3}{dt^2} = 0$$

$$2R_p^2K_b\frac{R_0}{R_1}\theta_0 - 2R_p^2K_b\theta_3 + 2R_p^2C_b\frac{R_0}{R_1}\frac{d\theta_0}{dt} - 2R_p^2C_b\frac{d\theta_3}{dt} + C_3\frac{d\theta_3}{dt}$$

$$+ J_3\frac{d^2\theta_3}{dt^2} = 0 \tag{11}$$

Finally rearranging equation (11) to get the second equation of motion of the laser beam manipulator

$$2R_p^2K_b\frac{R_0}{R_1}\theta_0 - 2R_p^2K_b\theta_3 + 2R_p^2C_b\frac{R_0}{R_1}\frac{d\theta_0}{dt} + (C_3 - 2R_p^2C_b)\frac{d\theta_3}{dt}$$

$$+ J_3\frac{d^2\theta_3}{dt^2} = 0 \tag{12}$$

In addition to the above two equations (8) and (12), the servomotor could be modelled as standard permanent magnet dc-motor differential equations. For a constant field current and armature control dc motor, the torque developed by the motor is described by the equation (13) below

$$T_m = K_m i_a \tag{13}$$

The speed of an armature-controlled dc servomotor is controlled by the armature voltage E_a. For a constant flux, the induced voltage E_b is directly proportional to the angular velocity dθ/dt. Therefore, the differential equation (14) for the armature current circuit is given by the Kirchoff's voltage law as below

$$L_a \frac{di_a}{dt} + R_a i_a + E_b = E_a \tag{14}$$

where $E_b = K_e \frac{d\theta_o}{dt}$

Based on the equations (8), (12), (13) and (14) above, the state-space equations are formulated and can be represented by five state variables and two control inputs as follows

$$\text{State variables} \quad X(t) = \begin{bmatrix} i_a & \theta_0 & \frac{d\theta_0}{dt} & \theta_3 & \frac{d\theta_3}{dt} \end{bmatrix}^T \tag{15}$$

$$\text{Control input} \quad U(t) = [E_a \quad T_f]^T \tag{16}$$

The detail state space model describing the overall dynamic system is described in Figure A of Appendix 1. This comprehensive state-space system description can be used to determine precisely the parameters that influence the dynamic performances of the laser beam manipulator for an accurate cutting process. Furthermore, various design parameters and motor selection can be made using this state space equation. Critical design parameters such as gear ratio, system bandwidth, pulley diameter, inertia, friction and PID control parameters can be determined and evaluated easily.

Simulation of Frequency Response

Frequency response analysis was carried out to determine the dynamic behaviour of the belt-driven laser manipulation system. Due to the elasticity and the damping of the belt, which is quite significant because of its long travel distance, it is desirable to predict its dynamic performance such as resonance, bandwidth and stability margin. This will ensure the speed and accuracy of the system to satisfy the design requirements. Two critical parameters, the effect of stiffness and the damping coefficient on the timing belt, were used to determine the performance of the timing-belt of the linear slide mechanism. An open-loop control strategy was used in the simulation of frequency response of the system. The simulation was done by using Matlab Simulink ® Software as shown in Figure 3.

Friction was assumed linear and any non-linear behaviour due to friction was not taken into consideration in the simulation. The belt stiffness K_b and belt-damping coefficient C_b were the only variables in the simulation. All other system parameters such as inertia, bearing damping coefficient and motor viscous friction were kept unchanged. If the mechanical property of the timing belt is

$$L_a \frac{di_a}{dt} + R_a i_a + E_b = E_a \tag{14}$$

where $E_b = K_e \frac{d\theta_o}{dt}$

Based on the equations (8), (12), (13) and (14) above, the state-space equations are formulated and can be represented by five state variables and two control inputs as follows

State variables $$X(t) = \begin{bmatrix} i_a & \theta_0 & \frac{d\theta_0}{dt} & \theta_3 & \frac{d\theta_3}{dt} \end{bmatrix}^T \tag{15}$$

Control input $$U(t) = [E_a \quad T_f]^T \tag{16}$$

The detail state space model describing the overall dynamic system is described in Figure A of Appendix 1. This comprehensive state-space system description can be used to determine precisely the parameters that influence the dynamic performances of the laser beam manipulator for an accurate cutting process. Furthermore, various design parameters and motor selection can be made using this state space equation. Critical design parameters such as gear ratio, system bandwidth, pulley diameter, inertia, friction and PID control parameters can be determined and evaluated easily.

Simulation of Frequency Response

Frequency response analysis was carried out to determine the dynamic behaviour of the belt-driven laser manipulation system. Due to the elasticity and the damping of the belt, which is quite significant because of its long travel distance, it is desirable to predict its dynamic performance such as resonance, bandwidth and stability margin. This will ensure the speed and accuracy of the system to satisfy the design requirements. Two critical parameters, the effect of stiffness and the damping coefficient on the timing belt, were used to determine the performance of the timing-belt of the linear slide mechanism. An open-loop control strategy was used in the simulation of frequency response of the system. The simulation was done by using Matlab Simulink ® Software as shown in Figure 3.

Friction was assumed linear and any non-linear behaviour due to friction was not taken into consideration in the simulation. The belt stiffness K_b and belt-damping coefficient C_b were the only variables in the simulation. All other system parameters such as inertia, bearing damping coefficient and motor viscous friction were kept unchanged. If the mechanical property of the timing belt is

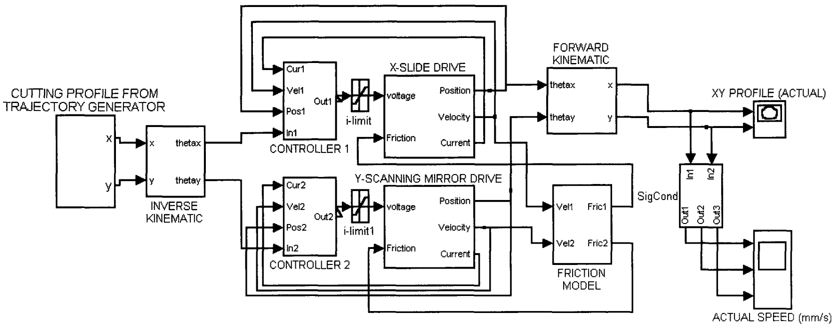

Figure 3: Simulink Block Diagram of the Laser Beam Manipulator

homogenous throughout its entire length, the belt stiffness or elasticity of the belt can be derived from this equation (17),

$$K_b = \frac{EA}{L} \tag{17}$$

Results of Frequency Response

By using the above equation (17), the belt stiffness is equal to 12.16 N/mm for a typical value of Young Modulus of timing belt E = 570 N/mm^2, cross sectional A = 16mm^2 and length L = 750 mm. In the first part of simulation, this value of belt stiffness remained constant while the value of the damping coefficient was increased from 0 to 1500 Ns/m. The frequency response results were plotted in form of bode diagrams as shown in Figure 4(a). As expected, the magnitude of the resonance was higher with the lower value of the belt damping coefficient. The belt-damping coefficient did not significantly affect significantly the frequency at which the resonance occurred. From the bode plot results, the bandwidth of the system was 29 rad/s with a phase margin of 290 degrees. The resonance frequency was 800 rad/s. Since the system bandwidth fell far below than resonance frequency, the system did not experience excessive vibration. Furthermore, the resonance was completely damped with the increasing value of damping coefficient. Normally, the actual value of the damping coefficient of the belt is approximately equal to 15000 Ns/m. This value of damping coefficient indicates that resonance will not happen within this system bandwidth. The bandwidth of the system can be improved significantly under the closed-loop control.

In the second part of simulation, the frequency response analysis was performed with no belt damping. The effect of different belt stiffness under no belt damping can be visualised in Figure 4(b). By changing the value of the

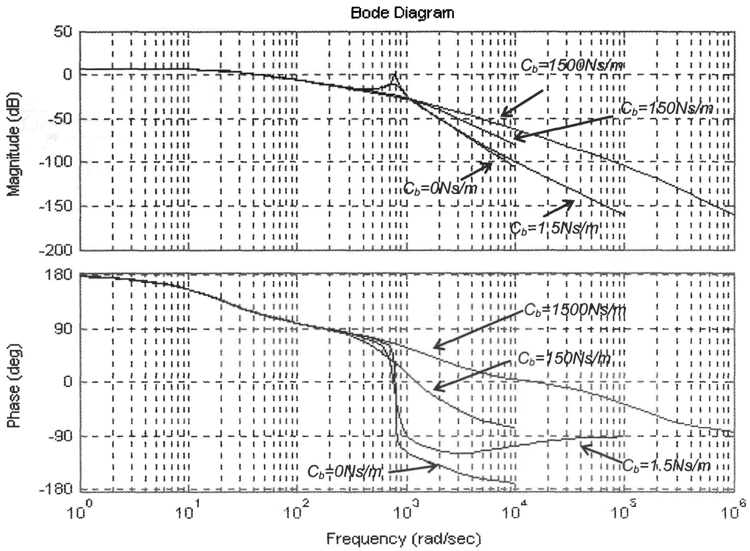

(a) Effect of Different Timing-Belt Damping Coefficients

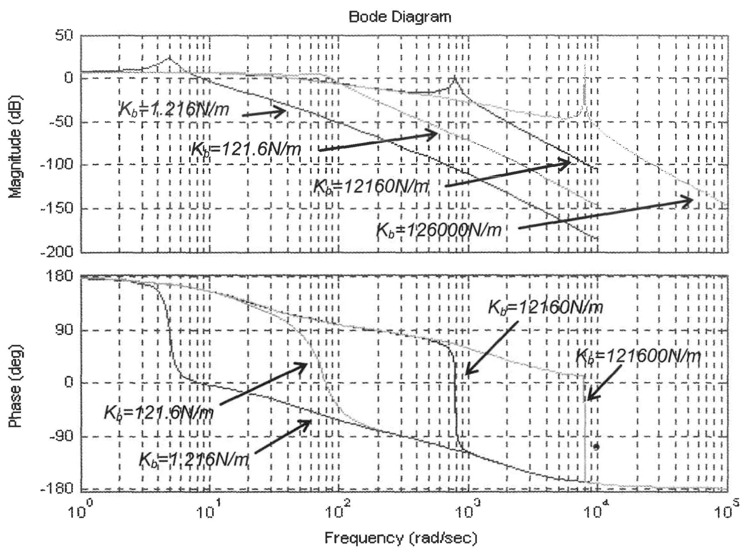

(b) Effect of Different Timing-Belt Stiffness

Figure 4: Frequency Response Analysis for the Laser-Beam Manipulator

belt cross-sectional area A and length L, four values of belt stiffness K_b were simulated. The values of stiffness K_b were increased from 1.2160 to 121600 N/m. The results showed that with a lower belt stiffness, the resonance will happen at a lower frequency. Even though a high value of the belt-damping coefficient will suppress the magnitude of resonance, it was important to select the belt stiffness where the resonance frequency was not within the range of system operating frequency. In this simulation, the specification of the other parameters are shown in Table 1.

Table 1: System Parameters for the Laser Beam Manipulator

Parameter	Specification		Parameter	Specification		Parameter	Specification
J_o	21.40 kgmm^2		J_3	550.00 kgmm^2		E	570 N/mm^2
C_o	10 μNms/rad		R_3	20 mm		A	16 mm^2
C_1	10 μNms/rad		C_3	10 μNMS/rad		L	750 mm
R_p	20 mm		E_a	24V		L_a	5 mH
K_m	90 mNm/A		K_e	108.2 mVs/rad		R_a	7.8 ohms

Conclusion

This paper introduces a comprehensive state space model of linear belt-driven mechanism in the development of rapid laser beam manipulator. This mathematic model is used to predict uncertain dynamics behaviour and resonance problems of the belt because of its elasticity that leads to vibrations, compliance, and higher friction. Frequencies response approach is used to determine the critical parameters of the system such as, phase margin, system bandwidth and the resonance of the system, for vibration suppression that can provide accurate control strategy of the manipulator. Instead of using complicated control strategies for vibration suppression, a simple controller such as PID controller was used to accurately plan the laser-beam trajectory within the system bandwidth to avoid exciting the resonance.

Acknowledgements

The authors would like to acknowledge the research grant given by the Festo Pty. Ltd. United Kingdom and Universiti Teknologi MARA, Malaysia.

References

[1] Smith, J., Lucas, J. and Steen, B. (1998). Vision-guided Laser Cutting of Embroidered Fabrics. *Journal of Engineering Technology, ISSN 1462-2165.* **1**(4): pp. 50-53.

[2] Dworkowski, R. and Wojcik, P. (1995). Computer Control for High-Speed, Precision Laser Cutting System. *Proceeding of the IEEE CCECE/CCGEI '95*, 5-8th September 1995, pp. 187-189, ISBN 0-7803-276679.

[3] Hafez, M., Benjamin, S. , Sidler, T. and Salathe, R. (2000). "Compact Laser System for Microprocessing applications". *Journal of Laser Applications, ISSN 1042-346X. Laser Institute of America.* 12(5): pp. 210-214.

[4] Ayub, M.A. and Jackson, M.R. (2002). 2D-Patterned Shape Cutting of Elastic Web Fabrics Using Vision Directed Laser Cutting: Design and Realiasation. *Proceeding of International Mechatronic Conference, Enschede, Netherlands.* ISBN 90365-17664 IEE, EEC mechatronics forum and University of Twente the Netherlands.

[5] Hace, A, Jezernik, K. and Sabanovic, A. (2005). SMC with disturbance Observer for a Linear Belt-Drive. *Proceedings of IEEE ISIE'05, June 20-23, 2005,* Dubrovnik, Crotia, pp. 1641-1646.

[6] Varanasi Kripa, K. and Nayfeh Samir, A. (2004). Damping of Vibration in Belt-Driven Motion Systems Using a Layer of Flow-Density Foam, *ASPE Proceedings, Control of Precision Systems*, April 19-20, 2004, Massachusetts Institute of Technology, Cambridge, Massachusetts.

[7] Hace, A., Jezernik, K. and Terbuc, M. (2005). Robust Motion Control Algorithm for a Linear Belt-Driven servomechanism. *Proceedings of IEEE ISIE'99, Ble, Slovenia.*

[8] Hace, A., Jezernik, K. and Sabanovic, A. (2005). Improved Design of VSS Controller for a Linear belt-driven Servomechanism. IEEE/ASME Transactions on Mechatronics, Vol. 10, No. 4, August 2005, ISSN 10834435.

[9] Kouhei Ohnishi, Masaaki Shibata and Toshiyuki Murakami (1996). Motion Control for Advanced Mechatronics, *IEEE IEEWASME Transactions On Mechatronics*, Vol. 1, No. 1, March 1996.

[10] Ayub, M.A. and Jackson, M.R. (2002). Simulation of Vision Driven On-line Trajectory Planning for Cutting 2D-Patterned Shape of Elastic Web Fabric. *Proceeding of 8th IEEE International Conference on Method and Models in Automation and Robotics,* MMAR2002, Szczecin, Poland. ISBN 88764-66-7. Polish Academic of Sciences Warsaw, IEEE Robotics and automation Society, Control System Society and Technical University of Szczecin Poland.

$$
\dot{X} = \begin{bmatrix}
\frac{R_a}{L_a} & 0 & -\frac{K_e}{L_a} & 0 & 0 \\
0 & 0 & 1 & 0 & 0 \\
\frac{K_m}{J_{o2}} & -\frac{2R_p^2 K_b \left[\frac{R_0}{R_1}\right]^2}{J_{o2}} & -\frac{C_o + \left[\frac{R_0}{R_1}\right]^2 \left[C_2 + 2R_p^2 C_b\right]}{J_{o2}} & -\frac{2R_p^2 K_b \left[\frac{R_0}{R_1}\right]}{J_{o2}} & -\frac{2R_p^2 C_b \left[\frac{R_0}{R_1}\right]}{J_{o2}} \\
0 & 0 & 0 & 0 & 1 \\
0 & -\frac{2R_p^2 K_b \left[\frac{R_0}{R_1}\right]}{J_3} & -\frac{2R_p^2 C_b \left[\frac{R_0}{R_1}\right]}{J_3} & -\frac{2R_p^2 K_b}{J_3} & -\frac{C_3 - 2R_p^2 C_b}{J_3}
\end{bmatrix}
\begin{bmatrix}
i \\ 0 \\ \frac{d\theta_0}{dt} \\ 3 \\ \frac{d\theta_3}{dt}
\end{bmatrix}
+
\begin{bmatrix}
\frac{1}{L_a} & 0 \\
0 & 0 \\
0 & -\frac{1}{J_{o2}} \\
0 & 0 \\
0 & 0
\end{bmatrix}
\begin{bmatrix}
E_a \\ T_f
\end{bmatrix}
$$

$$
\text{where } J_{02} = J_0 + J_2 \left[\frac{R_0}{R_1}\right]^2
$$

Figure A: Detail State-Space Model for the Laser Beam Manipulator